Survival of Activated Myofibroblasts in Canine Myxomatous Mitral Valve Disease and the Role of Apoptosis

Title:

Survival of Activated Myofibroblasts in Canine Myxomatous Mitral Valve Disease and the Role of Apoptosis

Authors: Rachel R. Blake[a], Greg R. Markby, Geoff J. Culshaw, Yolanda Martinez-Pereira, Chi-Chien Lu and Brendan M. Corcoran

Affiliation: Roslin Institute and Royal (Dick) School of Veterinary Studies, Roslin, Mid-Lothian Scotland, UK EH25 9RG

Corresponding author: Brendan M. Corcoran Brendan.Corcoran@ed.ac.uk +44 131 6506070

[a]Rachel R Blake. Present Address; Blake Scarsdale Vets, Riverside Road, Pride Park, Derby DE24 8HX

Abstract:

Myxomatous mitral valve disease (MMVD) is the single most important acquired cardiovascular disease of the dog. Much is known about the cellular changes and the contribution of activated myofibroblasts (valve interstitial cells (aVICs) to the valve extra-cellular matrix remodelling characteristic of the disease. However, little is known on how aVIC survival might contribute to disease pathogenesis. This study examined the temporal (disease severity-dependent) and spatial distribution of aVICs in MMVD valves, the expression of a range of apoptosis-related genes in cultured VICs from both normal (quiescent VIC (qVIC) and diseased (aVIC) valves, and the differential effects of doxorubicin treatment, as a trigger of apoptosis, on expression of the same genes. Activated myofibroblasts were identified in normal valves at the valve base only (the area closest to the annulus), and then became more numerous and apparent along the valve length as the disease progressed, with evidence of cell survival at the valve base. There were no significant differences in basal gene expression comparing qVICs and aVICs for *CASP3*, *FAS*, *BID*, *BAX*, *BCL2*, *CASP8*, *DDIAS*, *XIAP* and *BIRC5*. After doxorubicin treatment (2mM) for 8hrs there was significant difference ($P<0.05$) in the expression of *BID*, *BCL2*, *DDIAS*, and *CASP8*, but when assessed for interactions using a mixed model ANOVA only *CASP8* was significantly different because of treatment ($P<0.05$). These data suggest aVIC survival in MMVD valves may be a consequence of heightened resistance of aVICs

to apoptosis, but would require confirmation examining expression of the relevant proteins.
progression.

Key Words: Myxomatous mitral valve disease, valve interstitial cells, cell culture, activated myofibroblasts, apoptosis

1. Introduction:

Myxomatous mitral valve disease (MMVD) is the most common acquired cardiac disease of the dog and can lead to heart failure and death (Borgarelli and Haggstrom, 2010). The main feature of MMVD is destruction and disorganisation of the extracellular matrix (ECM), which is believed to be a consequence of valve interstitial cells in the valve stroma transitioning from a quiescent (qVIC) phenotype to activated myofibroblasts (aVIC; alpha smooth muscle actin positive (αSMA+)) (Aupperle and Disatian, 2012; Disatian et al., 2008; Hadian et al., 2007; Han et al., 2010; Han et al., 2008). A cardinal feature of MMVD is the increased numbers of aVICs, which correlates with disease progression and severity (Han et al., 2008; Lu et al., 2016). Activated myofibroblasts have previously been described adjacent to the myxomatous areas, with increased numbers in the sub-endothelium, but their extent and distribution throughout the entire length of the valve as disease progresses has not been reported (Han et al., 2008; Han et al., 2013; Lu et al., 2016). While several mechanisms have been suggested to contribute to the pathogenesis of MMVD, aVIC survival, either as a consequence of heightened senescence or reduced apoptosis (interconnected and related mechanisms), might be a contributing factor in the development and progression of MMVD (Surachetpong et al., 2013).

The activity of activated myofibroblasts in tissue repair is limited by the process of apoptosis (Hinz et al., 2007). When this does not occur persistent tissue remodelling can ensue resulting in tissue damage often typified by excessive fibrosis (Desmouliere et al., 1995; Linge et al., 2005). The survival of activated myofibroblasts as a driver of disease is of particular interest in myocardial infarction and hepatic, renal and lung fibrosis, because therapeutic interventions to control apoptosis and cell senescence could have major impact on the management of the these diseases, and by extension to

53 the management of MMVD (Hinz et al., 2012; Kisseleva et al., 2012; Lagares et al., 2017). For
54 example, the presence of activated myofibroblasts in histological samples of fibrotic myocardial
55 infarcts, several years after a known initiating event, is seen as indirect evidence of survival of
56 activated myofibroblasts (Willems et al., 1994).
57 The potential role of apoptosis in canine MMVD has been previously examined (Surachetpong et al.,
58 2013). Increased pro-apoptotic BCL-2-associated protein (BAX) and decreased anti-apoptotic B-cell
59 lymphoma 2 protein (BCL-2) expression, without changes in cleaved caspase 3 expression or TUNEL
60 (Terminal deoxynucleotidyl transferase-mediated deoxyuridine triphosphate nick-end labelling)
61 staining of apoptotic bodies have been reported in canine MMVD valves (Surachetpong et al., 2013).
62 While these data might suggest cells are in a primed pro-apoptotic state, it might also reflect the
63 complex interaction of pro-apoptotic factors and inhibitors of apoptosis. There is also evidence of
64 epigenetic control of apoptosis with reduced expression of miR-20a, miR-17 and miR-30d (pro-
65 apoptotic and anti-senescence) and increased expression of pro-senescent p21 in affected valves
66 (Karimian et al., 2016; Yang et al., 2018). Transcriptomic profiling of canine mitral valves has
67 identified changes in a range of apoptosis associated genes, including members of the BCL family
68 (*BCL6B* and *9*), *CASP4* and *CASP8*, *DED* (death effector domain), *DAD1* (defender against apoptotic
69 cell death), and various angiopoietin and pleiotrophin genes (Lu et al., 2015b). Transcriptomic
70 profiling has also found increased expression of *CDKN1A* and *CDKN2A*, which encode for the proteins
71 P21 and P16 respectively (Lu et al., 2015b). These cyclin-depended kinase inhibitors are important in
72 the control of cell senescence, and may have a role alone, or in tandem with apoptotic mechanisms,
73 in controlling activated myofibroblast survival in MMVD (Childs et al., 2014).
74 The control of apoptosis is complex and consists of intrinsic (stressor-induced mitochondrial
75 damage) and extrinsic (tumour necrosis factor family member death ligand-induced; TNF) pathways,
76 and has been reviewed extensively. These pathways converge to activate the executioner caspases
77 3, 6 and 7. The important proteins in the pathways include the caspases, FAS-ligand (CD95) and BH3
78 interacting-domain death agonist (BID) (pro-apoptotic), BCL-2 family members (both pro- and anti-),

X-linked inhibitor of apoptosis (XIAP) (anti-), inhibitor of apoptosis proteins (IAP) family members such as survivin (*BIRC5*, anti-), and FADD-like IL-1β-converting enzyme-inhibitory protein (c-FLIP) and DNA damage induced apoptosis suppressor protein (DDIAS) (anti-). The important BCL-2 family are regulated by several pathways, including growth factors affecting PI3K, ERK 1/2, JAK/STAT and NFκβ, and this may be important considering the potential role of TGFβ and 5-HT signalling in MMVD pathogenesis (Disatian et al., 2010; Disatian and Orton, 2009; Driesbaugh et al., 2018; Tan et al., 2019).

We hypothesised that there is survival of activated myofibroblasts in canine MMVD valves and that this, in part, can be explained by a defect in the activation and progression of apoptotic pathways. To investigate this hypothesis, we examined the spatial and temporal distribution of aVICs in mitral valves to confirm survival, and then examined the expression of apoptotic genes by qVIC and aVICs in cell culture, before and after stimulation with doxorubicin (Tan et al., 2019).

2. Materials and Methods:

2.1 Tissue samples

Dogs were euthanased with an intravenous pentobarbitone over-dose with full owner consent and the study was approved by the R(D)SVS Veterinary Ethics in Research Committee. No dogs were euthanased for the purpose of the study. Dogs with severe MMVD were typically euthanased because of intractable heart failure, and normal, mild and moderately affected dogs for non-cardiac reasons. Valves were collected from a range of dog breeds of varying ages and were graded independently by two of the authors (C-CL & BMC) as normal, mild, moderate or severely affected using a modification of the Whitney system (Whitney, 1974). A selection of valves were then processed for immunostaining (n=4 per grade; combination of elderly Cavalier King Charles Spaniels, elderly mixed breed dogs and young adult mixed breed dogs and beagles) or for valve interstitial cell culture (n= 11; combination of mixed breed dogs and beagles). For tissue sectioning, valves were washed with PBS, immersed in 4% paraformaldehyde and fixed at 4^{o}C for 36 hours, and then rinsed in PBS and stored in 70% ethanol at 4^{o}C until required. Samples for sectioning were collected from

105 the mid-point of the anterior leaflet of normal valves and the approximate same position from
106 grossly obvious areas of pathology on the anterior leaflet of diseased valves. Samples were paraffin-
107 embedded and four consecutive 5µm thick sections were collected onto gelatin coated slides.

108 ***2.2. Valve interstitial cell (VIC) culture***

109 Valve interstitial cells (MMVD n=6; normal n=5) were collected for culture from excised valves using
110 previously described methods, except the culture media (Dulbecco's Modified Eagle Medium
111 (DMEM); Life Technologies, U.S.A) contained 2% instead of standard 10% v/v FBS in order to
112 preserve cell phenotype (Latif et al., 2015; Liu et al., 2015; Tan et al., 2019). Cells were seeded in T75
113 culture flasks (ThermoScientific) in 15ml of DMEM, with FGF-2 only added at that point, and
114 incubated at 37˚C in 5% CO_2. Culture medium was changed every 2-3 days, and once confluence was
115 reached the cells were harvested by trypsinization (TrypLE™ Express; Life Technologies). Cell pellets
116 was either re-suspended in culture medium for continued culture, or prepared for storage at -150˚C.
117 Cells were used no later than passage five.

118 ***2.3. Indirect immunofluorescence Immunohistochemistry***

119 A standard protocol was used as previously described (Lu et al., 2016).For antigen retrieval, sections
120 were heated in citrate buffer for 5 minutes at 120˚C. Slides were mounted in Sequenza cassettes
121 (Thermo Scientific, Shandon Sequenza Immunostaining Cassettes) with 200 µm of 0.5% PBS-
122 Tween20. Permeabilization and non-specific-blocking of antigens were performed with 10% goat
123 serum (diluted in 0.5% Tween 20) (Vector Laboratories Inc.) for 30 minutes at room temperature.
124 Sections were then incubated for 60 minutes at room temperature with mouse monoclonal anti-
125 αSMA antibody at 1:400 dilution (Sigma; cat. no. A2547) washed with 0.5% PBS-Tween20 and
126 incubated for 30 minutes at room temperature with a goat anti-mouse fluorescein-conjugated
127 secondary antibody at 1:1000 dilution (Invitrogen; Alexafluor, cat. no. A10667). Slides were mounted
128 in medium containing the nuclear counterstain DAPI (ProLong Gold Antifade Reagent, Invitrogen),
129 viewed immediately andor stored at -20˚C. Images were collected using a light fluorescence

microscopy (Leica-DMLB) and tile-scanning was performed using a Zeiss LSM-710 confocal microscope. The images were then assessed qualitatively for cell density and cell distribution.

2.4. Cell RNA extraction, quantification and quality assessment

Cell lysis was performed using the QIAshredder homogenizer (QIAGEN, Germany) and RNA was extracted from frozen cell pellets using the QIAGEN RNeasy Mini Kit (QIAGEN) according to the manufacturer's protocol. Quantification of RNA and contamination assessment was performed using the Nanodrop 1000 Spectrophotometer Version 3.7.1 (Thermo Fisher Scientific). Samples were then promptly stored at -70˚C for batch complementary DNA (cDNA) generation.

2.5. Reverse transcription, primer design and real-time quantitative polymerase chain reaction (RT-qPCR)

Reverse transcription of RNA to cDNA was performed using the Superscript III™ Reverse Transcriptase kit (Invitrogen). Two primer pairs for each of *BCL-2*, *DDIAS*, *BID* and *FAS* one primer pair for *CASP8*, *CASP3*, *BIRC5*, *XIAP* and *BAX* were designed using Primer3web version 4.1.0 software (Untergasser et al., 2012, Koressaar and Remm, 2007) based on canine sequences from the Ensembl database. Second primer sequences for each of CASP8, *CASP3*, *BIRC5*, *XIAP* and *BAX* have been previously reported (Del Puerto et al., 2010, Yamazaki et al., 2013, Meichner et al., 2016). Primers for *ACTA2* (αSMA) and *TAGLN* (SM22α) had previously been designed and optimized (Markby 2018). Expression of these genes in normal and diseased VICs was analysed at baseline in order to validate cell phenotype, with high *ACTA2* and *TAGLN* expression expected in diseased VICs, but not in healthy VICs. Primers for the three reference genes used (GAPDH, MRPS25, RPL32) had previously been validated (Liu et al., 2015). Primer sequences are shown in Table 1.

The Takyon™ Low Rox SYBR® Mastermix dTTP Blue kit (Eurogentec, Belgium) was used to perform RT-qPCR in 96-well PCR plates (ThermoScientific). RT-qPCR was then performed using the Stratagene MxPro Mx3000P (Agilent Technologies, U.S.A.).

2.6. Doxorubicin induction of apoptosis

Time-course experiments were undertaken to establish optimal timing for detection of apoptosis. One each of a normal and diseased VIC culture (passage 4) were tested with a REM134 canine mammary carcinoma cell line (passage 43). Cells were grown for 48hrs at 37°C in 5%CO_2 and treated with 2mM doxorubicin hydrochloride (Medac, GmbH, 2mg/ml) (Forterre et al., 2011). Cells were harvested at 0, 2, 4, 8, 16 and 24hrs and examined for expression of *BCL-2*, *BAX*, *BIRC5*, *CASP3* and the reference genes *GAPDH*, *MRPS25*, *RPL32*. Based on these results, experiments were undertaken in all the VIC samples, harvesting at 0, 4, 8 and 24hrs and examined for the expression of *BCL-2*, *BAX*, *BIRC5*, *CASP3, CASP8*, *DDIAS*, *BID*, *XIAP* and *FAS*.

2.7. Modified ethidium homodimer and acridine orange viability assay

Because doxorubicin treatment was likely to cause cell necrosis, this assay was used to determine the number of live, apoptotic and necrotic cells. VICs from four dogs were prepared and treated with doxorubicin in 96 well plates. A solution of ethidium homodimer inn DMSO (EH) and acridine orange (AO) (Invitrogen), each at 100µg/ml, was prepared in PBS (Ribble et al., 2005). Well plates were centrifuged at 453g for 5 minutes and 8µl of the AO/EH solution added to the 100ml of culture media in each well, giving a final concentration of 14.8µg/ml. After 2 minutes cells were examined by fluorescent microscopy and three photo-micrograph obtained, 100 cells counted in each frame and the percentage of live, dead and apoptotic cells calculated.

2.8. Statistical analysis

Statistical analysis was performed using Minitab 17 Statistical Software and IBM SPSS Statistics 24. Normality was assessed visually and using the Anderson-Darling test. A 2-sample t-test (for parametric data) or a Mann-Whitney U test (for non-parametric data) was used to compare ΔCt values to investigate for differences in gene expression between normal and diseased VIC groups at baseline. A one-sample t-test was used to compare individual ΔCt values of diseased VICs with the group of normal VICs when investigating individual genotypes. A mixed model analysis of variance (ANOVA) was used to investigate changes in gene expression following induction of apoptosis. Delta Ct was considered the dependent variable, VIC type (healthy or diseased) and treatment status were

considered fixed effects and dog ID was a random effect. Standardized residuals were analysed visually for normality and found to be adequate in all cases. Significant interactions were analysed using an independent t-test. A value of $p<0.05$ was considered significant.

3. Results

A clear change in the density and distribution of activated myofibroblasts was identified, with increasing number of αSMA+ cells as the disease progresses, and along the length of the leaflet from distal zone to base (Fig. 1). In normal leaflets, αSMA+ cells were identified as a single layer only in the basal zone with some extension into the mid zone, and only on the atrial side of the leaflet. In mild to moderately diseased valves, additional linear clusters of αSMA+ cells were found extending to the valve edge, again primarily towards the atrial side in the sub-endothelium, and with retention of positive staining in the basal zone as seen in the normal valves. There was further increase in αSMA+ cells in severely affected leaflets, with extension to the ventricular side and deeper within the myxomatous core. Again positive staining of the mid and basal zone was retained.

To check for accuracy of cell phenotype expression of *ACTA2* and *TAGLN* was measured in all cells and two diseased samples had reduced gene expression, and this was factored into the analyses.

Cells continued to grow after doxorubicin treatment with qVICs and aVICs retaining their characteristic morphology, as did the number of dead cells which appeared rounded, shrunken and detached from the culture flask base (Fig. 2). EH/AO staining identified a decrease in the proportion of live cells and an increase in apoptotic and necrotic cells at 8hrs for both qVICs and aVICs, but an increased percentage of apoptotic cells was also seen in untreated samples at 8hrs (Fig. 3). Although there was a -1.05 (XIAP) to 2.43 (DDIAS) fold change difference comparing qVICs and aVICs, in baseline expression for the apoptotic-related genes examined, no differences achieved statistical significance (Table 2). With doxorubicin treatment of qVIC (n=5) and aVIC (n=6) samples at 8hrs, there was a statistically significant increase in pro-apoptotic *BID* and *CASP8* and a decrease in anti-apoptotic *BCL2* and *DDIAS* compared to untreated controls ($p<0.05$) (Table 3 and Fig. 4). When

assessed for interaction using the mixed-model ANOVA, only *CASP8* was significantly decreased in the aVICs ($p<0.05$) (Table 3).

Removing the two aVIC samples with low *ACTA2* and *TAGLN* expression, significant differences in expression of *BID*, *BCL2* and *DDIAS* were retained, but not for *CASP8*. Gene expression at 4hrs post-treatment identified a significant decrease in pro-apoptotic *FAS* and *CASP8* and anti-apoptotic *BCL2* and *DDIAS* in aVICs, and a decrease in *CASP8* and *DDIAS* in qVICs ($p<0.01$), with interaction identified for BCL2 and DDIAS ($p<0.05$). While there was no overall effect of doxorubicin on *CASP3* expression, there was a crossover interaction with the mixed-model ANOVA, which *post hoc* analysis identified as an increase in *CASP3* at 4hrs in control aVICs ($p<0.05$). Untreated qVIC and aVIC controls also showed changes at 4hrs, including increased *FAS* and *BID* in both and increased *DDIAS* in diseased and *BCL2* in normal VICs ($p<0.05$). Removing the two aVIC samples with low *ACTA2* and *TAGLN* expression removed the interaction for *BCL2* and *DDIAs*, with only the treatment having a continual significant effect. While untreated VICs continued to grow, by 24hrs the majority of cells in the doxorubicin treated qVIC and aVIC groups appeared necrotic.

4. Discussion

This study identified a temporal and spatial pattern of activated myofibroblasts in canine MMVD characterised by increasing numbers and widening distribution of activated cells as the disease progressed. While it cannot be stated with certainty that the αSMA+ cells in the valve base and mid-zones seen across all grades of disease is due to survival, the consistency of the finding in all dogs examined would be highly supportive of this conclusion. This suggests cell survival typical of heightened cell senescence and/or reduced apoptosis is found in MMVD. The appearance of aVICs is a hallmark of MMVD, but has been presumed to be closely associated with myxomatous pathology as it develops (Disatian et al., 2008; Han et al., 2008; Lu et al., 2016). While this is likely to be the case, aVICs are first identified in the basal zone and remain there throughout the natural progression of the disease. The extent to which aVIC numbers and distribution is a combination of cell migration, proliferation or transformation of the resident qVIC population is unknown. Increased expression of

Ki67 has been reported suggesting proliferation is involved, but endothelial-to-mesenchymal transition might also contribute to the aVIC population (Lu et al., 2015a; Lu et al., 2016). There are no reports of cells being recruited from the circulating fibrocyte pool in dogs, but CD34+ cells have been identified in human MMVD, suggesting this may be a source (Barth et al., 2005). Further studies for markers of apoptosis (and senescence) are now needed examining aVICs at all locations in valve tissue and at all disease time-points.

Survival of activated myofibroblasts is well recognised in other diseases, and for some this results in continual pathological changes, while for others pathology is not progressive (Desmouliere et al., 1995; Hinz et al., 2012; Linge et al., 2005; Willems et al., 1994). Similarly, survival of aVICs, and their accumulation in the mitral valve is an important process in the development and progression of MMVD, and may represent a potential therapeutic target for disease management.

Differential expression of pro- and anti-apoptotic genes was not identified in VICs from normal and disease valves. However, with doxorubicin aVICs differentially expressed *CASP8* suggesting that aVICs have some resistance to normal apoptosis. Caspase 8 is the final enzyme in the extrinsic apoptotic pathway activating the executioner caspases as well as linking to and activating the intrinsic apoptotic pathway. Inhibitors of caspase 8 activity include DDIAS, which promotes phosphorylation, ubiquitination and degradation of the caspase 8 enzyme, but DDIAS was also found to be decreased in doxorubicin treated VICs (Im et al., 2018). However, DDIAS acts post-translationally to control caspase 8 expression and so would not have an effect on the level of gene expression, but only on protein quantity and activity. An additional pro-survival mechanism for aVICs might be increased expression of *BIRC5*, which was found increased in the sub-analysis, although this did not achieve significance. *BIRC5* encodes for the protein survivin, which inhibits the final steps of the apoptotic pathway, aiding XIAP in inhibiting executioner caspases and caspase 9 (Jaiswal et al., 2015).

Doxorubicin causes apoptosis in cardiomyocytes and cancer cells, can induce senescence, and appeared a reasonable choice to see if drug-triggering could be used to identify differences in

apoptotic signals comparing qVICs and aVICs (Wang et al., 2004). For qVICs and aVICs there were similar changes in the genes involved in the earlier stages of the apoptotic signalling pathway, including increase in pro-apoptotic *BID* and decrease in anti-apoptotic *BCL2* and *DDIAS*. Diseased VICs did not demonstrate a significantly more pro-apoptotic state than healthy VICs. This contrasts somewhat with previous reports looking at protein expression for BAX, BCL-2 and cleaved caspases in MMVD valves (Surachetpong et al., 2013). Furthermore, transcriptomic profiling of canine aVICs has identified several gene changes associated with down-regulation of apoptotic pathways and heightened senescence (Tan et al., 2019).

While it was anticipated that doxorubicin treatment would induce more clear changes in gene expression comparing the two VIC populations, this may not have happened due to the greater importance of post-translational changes (Jager and Zwacka, 2010). This is particularly true in the case of caspases, as they require cleavage or dimerization to be activated (Plati et al., 2011). Further work is now needed to examine baseline protein expression in the two cell types, and after doxorubicin exposure, before the data presented here can be interpreted as convincing proof of apoptosis. Use of TUNEL staining, as a commonly used measure of apoptosis, would also be need to confirm and compliment the EH/AO findings

The possible contribution of variance in cell phenotype also needs to be considered, such that cells even from diseased valves can be at varying stages of apoptosis, necrosis or senescence, and the summative gene expression (up or down) resulting in no change in the level of gene expression. This confounder was minimised to a certain extent in this study. Lastly, doxorubicin can also induce TGF-β signalling that can transform qVICs to aVICs in heart valves and fibroblasts to myofibroblasts in myocardium, and may have had a similar effect transitioning qVICs to aVICs (Tan et al., 2019). While we assessed changes in cell phenotype based on morphology we did not examine changes in *ACTA2* or *TAGLN* expression in the treated qVICs. Nevertheless, the time course experiments and the examination of cells using EH/AO suggested doxorubicin was having a differential effect on the aVICs.

5. Conclusion

It has previously been suggested that cells in MMVD valves are possibly in a pro-apoptotic state, but the gene expression shown here, and the temporal and spatial distribution of aVICs in normal and affected valves suggest arrested apoptosis might contribute to the appearance and survival of activated myofibroblasts in canine MMVD. Further work is now required to confirm if this is the case by examining expression of cleaved and activated proteins in activated myofibroblasts.

Conflict of interest

The authors declare that there are no conflicts of interest.

Acknowledgements

We wish to acknowledge Dr Lisa Pang for her advice on the use of doxorubicin in this study and Dr Karen Tan for her advice on cell culture protocols.

Figure Legends

Figure. 1. Representative photomicrographs of alpha smooth muscle actin (αSMA+) staining in canine mitral valves at different stages of myxomatous degeneration. Upper part of each panel, αSMA (green) showing valve interstitial cell location, and lower part αSMA/DAPI (blue) showing the valve shape and extent of pathology. The intense staining (non-specific) at the far right each photomicrograph of each valve is the atrial myocardium. Bar =200µm.

Figure 2. Representative photomicrographs of cultured REM134 canine mammary carcinoma cell line cells, normal valve interstitial cells (Normal VIC) and diseased valve interstitial cells (Diseased VIC) prior to and after 2mM doxorubicin hydrochloride treatment. For each cell type there is an increase in cell numbers but also an increase in the number of dead cells. Bar = 100µm.

Figure 3. Representative immunofluorescent photomicrographs of ethidium homodimer and acridine orange staining illustrating live (L; green), dead (red) and apoptotic (green nucleus) cells in

normal and diseased valve interstitial cell cultures at 0hrs and at 8hrs with or without 2mM doxorubicin hydrochloride treatment. Bar = 100µm.

Figure 4. Difference in ΔCt between 0 hour and 8 hour for the genes *CASP3*, *FAS*, *BID*, *BAX*, *BCL2*, *CASP8*, *DDIAS*, *XIAP* and *BIRC5* plotted for diseased (D) and healthy (N) VICs, both treated (2 mM doxorubicin) (T – blue) and untreated (UT – green). An increase in the difference in ΔCt above 0 suggests a decrease in gene expression at 8 hours compared to 0 hours.

Gene	Forward primer 5'-3' Reverse primer 5'-3'	Product length (bp)	Tm (˚C)	Reaction efficiency (%)	Slope	R2
BCL-2	ACAACATCGCCCTGTGGAT	133	62	109.9	-3.105	0.96
	AGCCAGGAGAAGTCAAACAGA					
BAX	CCTCTTCTACTTTGCCAGCA	93	61	103.7	-3.237	0.98
	AAGTCCAGTGTCCAGCCCAT					
BIRC5	ACTGGACAAAGAAAGAGCCAAG	84	62	96.7	-3.404	0.96
	ACTTTCTTTGCGGTCTCTTCG					
CASP3	TTCATTATTCAGGCCTGCCGAGG	83	59	91.6	-3.542	0.99
	TTCTGACAGGCCATGTCATCCTCA					
CASP8	ACAAGGGCATCATCTATGGCTCTGA	70	61	103.2	-3.247	0.99
	CCAGTGAAGTAAGAGGTCAGCTCAT					
DDIAS	GAAACACTGGACCATGATGCA	122	62	102	-3.275	0.87
	TCTGAACCTTGTCCGTGTTG					
BID	AGGACTACGACGATGAGCTG	150	59	94.4	-3.463	0.96
	TGTGATCCATCCTGTCCCCT					
XIAP	GTGCTCAGAAAGACCATACACA	149	58	94.1	-3.473	0.99
	GCAAGGAATGAAAACCACAGC					
FAS	AGATCGGGTAGGAACGTCAC	141	59	106.6	-3.173	0.8
	ACAGTGTGATTTACCCGCAT					
ACTA2	CGGCTACTCCTTTGTGACG	100	58	102.2		

	CGTGGCCATCTCGTTCTC			
TAGLN	GACATGTTCCAGACCGTCGA	199	59	106.7
	CAATGACGTGCTTTCCCTCC			

Table 1. Reference and target gene forward and reverse primer sequences, product length, optimal annealing temperature and reaction efficiency.

Gene	Fold Change	P-value
BID	0.98	0.977
FAS	1.22	0.722
CASP3	0.91	0.883
BAX	0.98	0.964
CASP8	1.2	0.681
BCL2	0.74	0.492
BIRC5	1.58	0.631
DDIAS	2.43	0.363
XIAP	0.95	0.939

Table 2. Fold change, with associated p-values, comparing baseline gene expression between normal and diseased VICs.

Gene	Diseased vs healthy p-value	Treated vs untreated p-value	Interaction	Fold change healthy VIC (0 hour to 8 hour treated)	Fold change diseased VIC (0 hour to 8 hour treated)
CASP3	0.224	0.378	0.979	1.08	0.97
FAS	0.105	0.144	0.214	1.01	0.52
BID	0.960	0.016*	0.790	1.13	1.07
BAX	0.678	0.952	0.154	1.02	0.84
BCL2	0.413	0.003*	0.299	0.75	0.67
CASP8	0.195	0.016*	0.015*	0.94	0.54
DDIAS	0.197	<0.001*	0.390	0.37	0.25
XIAP	0.413	0.113	0.965	0.85	0.74
BIRC5	0.756	0.052	0.425	1.36	1.27

Table 3. Mixed-model ANOVA comparison of gene changes in response to doxorubicin at 8 hours in normal and diseased VICs.*statistically significant p<0.05.

Figure 1.

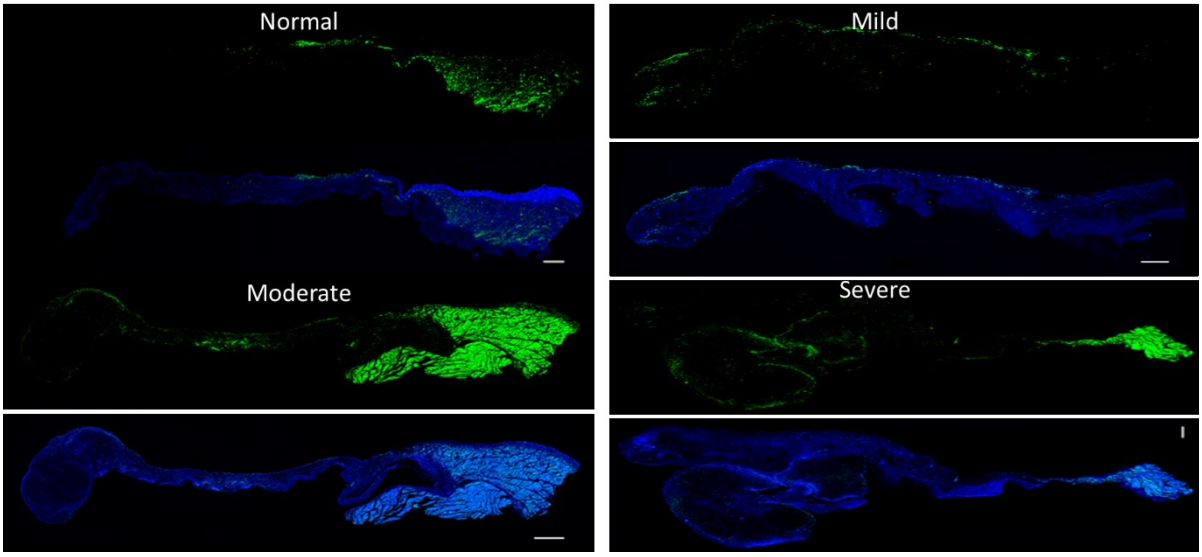

Figure 2.

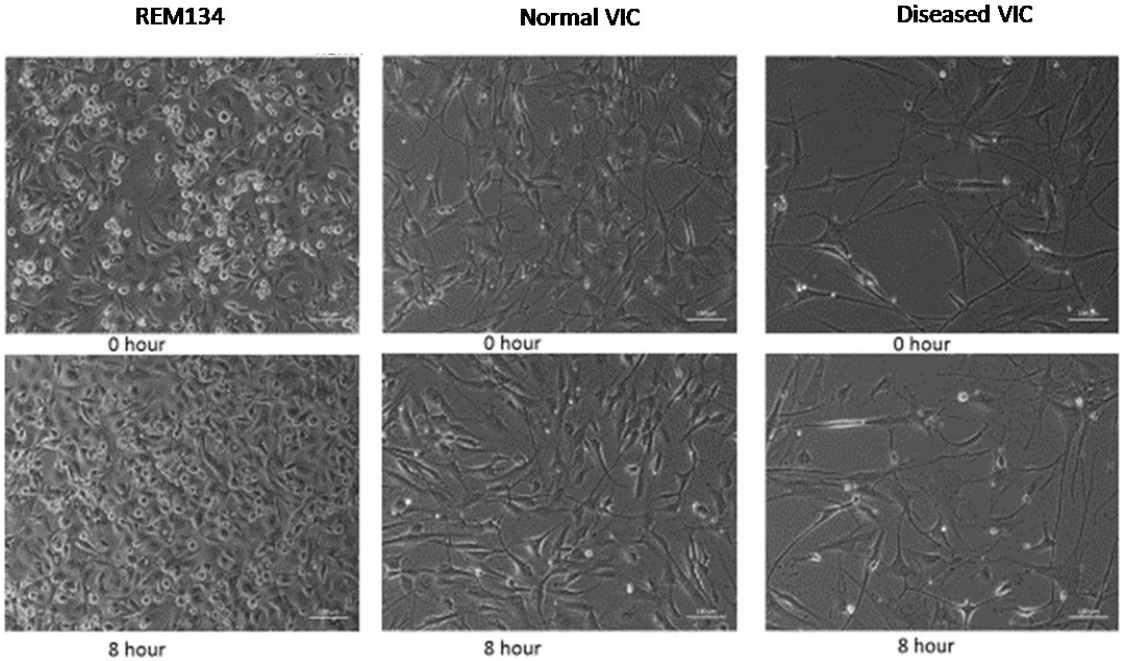

337 **Figure 3.**

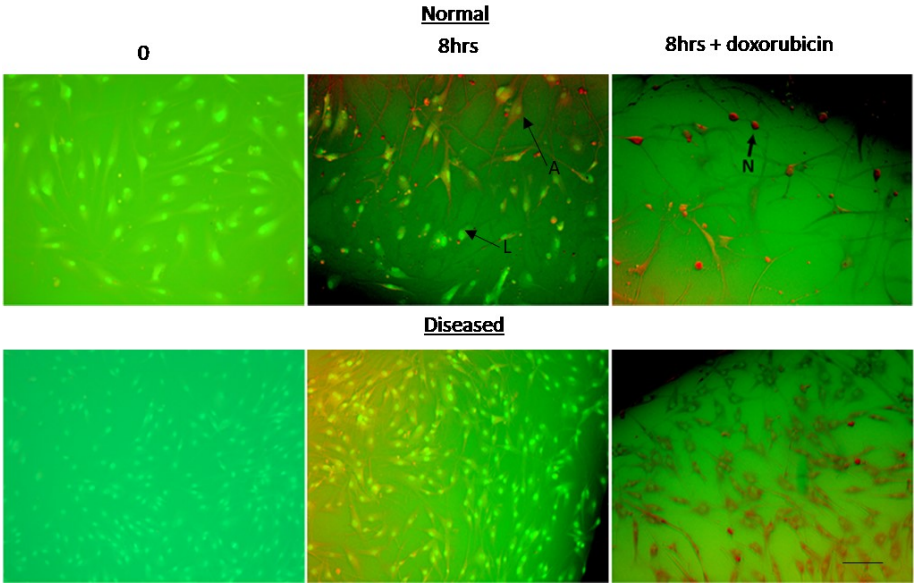

338

339 **Figure 4.**

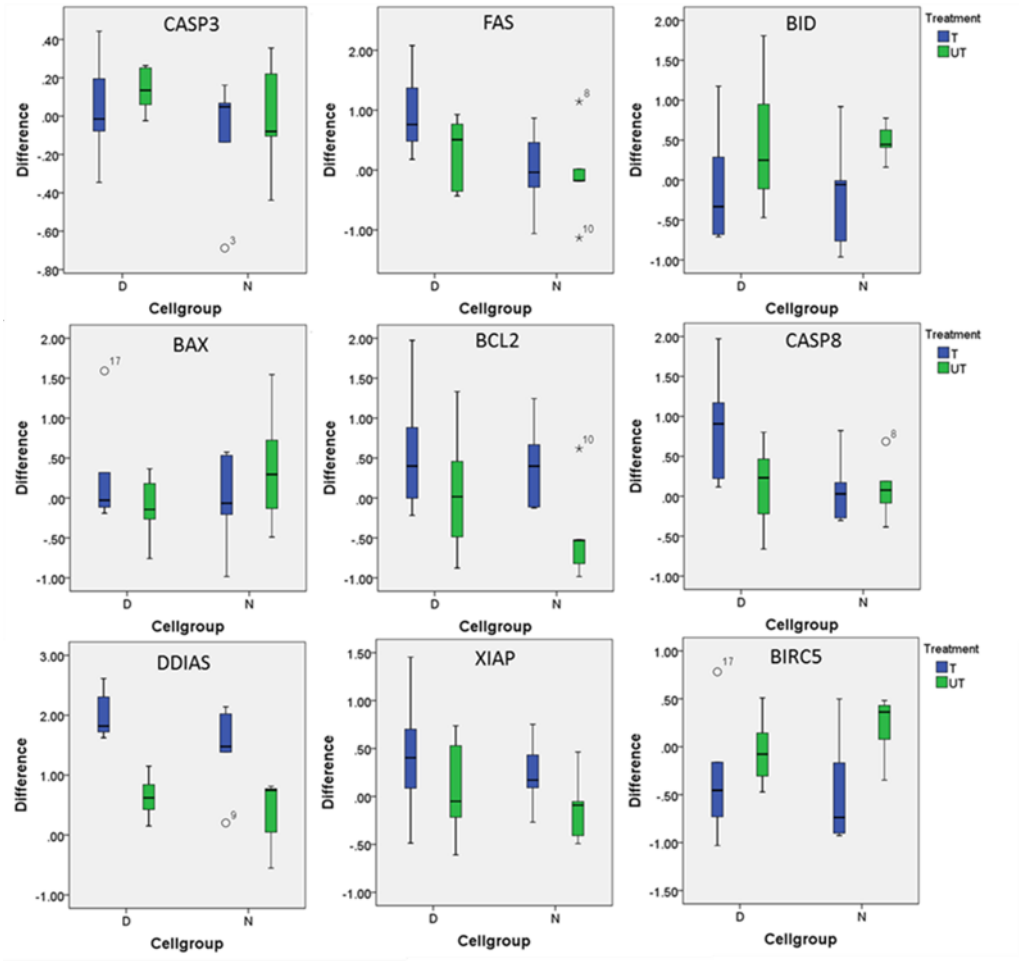

340

References

Aupperle, H., Disatian, S., 2012. Pathology, protein expression and signaling in myxomatous mitral valve degeneration: comparison of dogs and humans. J Vet Cardiol 14, 59-71.

Barth, P.J., Koster, H., Moosdorf, R., 2005. CD34+ fibrocytes in normal mitral valves and myxomatous mitral valve degeneration. Pathol Res Pract 201, 301-304.

Borgarelli, M., Haggstrom, J., 2010. Canine degenerative myxomatous mitral valve disease: natural history, clinical presentation and therapy. Vet Clin North Am Small Anim Pract 40, 651-663.

Childs, B.G., Baker, D.J., Kirkland, J.L., Campisi, J., van Deursen, J.M., 2014. Senescence and apoptosis: dueling or complementary cell fates? EMBO Rep 15, 1139-1153.

Desmouliere, A., Redard, M., Darby, I., Gabbiani, G., 1995. Apoptosis mediates the decrease in cellularity during the transition between granulation tissue and scar. Am J Pathol 146, 56-66.

Disatian, S., Ehrhart, E.J., 3rd, Zimmerman, S., Orton, E.C., 2008. Interstitial cells from dogs with naturally occurring myxomatous mitral valve disease undergo phenotype transformation. J Heart Valve Dis 17, 402-411; discussion 412.

Disatian, S., Lacerda, C., Orton, E.C., 2010. Tryptophan hydroxylase 1 expression is increased in phenotype-altered canine and human degenerative myxomatous mitral valves. J Heart Valve Dis 19, 71-78.

Disatian, S., Orton, E.C., 2009. Autocrine serotonin and transforming growth factor beta 1 signaling mediates spontaneous myxomatous mitral valve disease. J Heart Valve Dis 18, 44-51.

Driesbaugh, K.H., Branchetti, E., Grau, J.B., Keeney, S.J., Glass, K., Oyama, M.A., Rioux, N., Ayoub, S., Sacks, M.S., Quackenbush, J., Levy, R.J., Ferrari, G., 2018. Serotonin receptor 2B signaling with interstitial cell activation and leaflet remodeling in degenerative mitral regurgitation. J Mol Cell Cardiol 115, 94-103.

Forterre, S., Zurbriggen, A., Spreng, D., 2011. In vitro effect of different mediators of apoptosis on canine cranial and caudal cruciate ligament fibroblasts and its reversibility by pancaspase inhibitor zVAD.fmk. Vet Immunol Immunopathol 139, 264-270.

Hadian, M., Corcoran, B.M., Han, R.I., Grossmann, J.G., Bradshaw, J.P., 2007. Collagen organization in canine myxomatous mitral valve disease: an x-ray diffraction study. Biophysical journal 93, 2472-2476.

Han, R.I., Black, A., Culshaw, G., French, A.T., Corcoran, B.M., 2010. Structural and cellular changes in canine myxomatous mitral valve disease: an image analysis study. J Heart Valve Dis 19, 60-70.

Han, R.I., Black, A., Culshaw, G.J., French, A.T., Else, R.W., Corcoran, B.M., 2008. Distribution of myofibroblasts, smooth muscle-like cells, macrophages, and mast cells in mitral valve leaflets of dogs with myxomatous mitral valve disease. Am J Vet Res 69, 763-769.

Han, R.I., Clark, C.H., Black, A., French, A., Culshaw, G.J., Kempson, S.A., Corcoran, B.M., 2013. Morphological changes to endothelial and interstitial cells and to the extra-cellular matrix in canine myxomatous mitral valve disease (endocardiosis). Vet J 197, 388-394.

Hinz, B., Phan, S.H., Thannickal, V.J., Galli, A., Bochaton-Piallat, M.L., Gabbiani, G., 2007. The myofibroblast: one function, multiple origins. Am J Pathol 170, 1807-1816.

Hinz, B., Phan, S.H., Thannickal, V.J., Prunotto, M., Desmouliere, A., Varga, J., De Wever, O., Mareel, M., Gabbiani, G., 2012. Recent developments in myofibroblast biology: paradigms for connective tissue remodeling. Am J Pathol 180, 1340-1355.

Im, J.Y., Kim, B.K., Lee, J.Y., Park, S.H., Ban, H.S., Jung, K.E., Won, M., 2018. DDIAS suppresses TRAIL-mediated apoptosis by inhibiting DISC formation and destabilizing caspase-8 in cancer cells. Oncogene 37, 1251-1262.

Jager, R., Zwacka, R.M., 2010. The enigmatic roles of caspases in tumor development. Cancers (Basel) 2, 1952-1979.

Jaiswal, P.K., Goel, A., Mittal, R.D., 2015. Survivin: A molecular biomarker in cancer. Indian J Med Res 141, 389-397.

Karimian, A., Ahmadi, Y., Yousefi, B., 2016. Multiple functions of p21 in cell cycle, apoptosis and transcriptional regulation after DNA damage. DNA Repair (Amst) 42, 63-71.
Kisseleva, T., Cong, M., Paik, Y., Scholten, D., Jiang, C., Benner, C., Iwaisako, K., Moore-Morris, T., Scott, B., Tsukamoto, H., Evans, S.M., Dillmann, W., Glass, C.K., Brenner, D.A., 2012. Myofibroblasts revert to an inactive phenotype during regression of liver fibrosis. Proc Natl Acad Sci U S A 109, 9448-9453.
Lagares, D., Santos, A., Grasberger, P.E., Liu, F., Probst, C.K., Rahimi, R.A., Sakai, N., Kuehl, T., Ryan, J., Bhola, P., Montero, J., Kapoor, M., Baron, M., Varelas, X., Tschumperlin, D.J., Letai, A., Tager, A.M., 2017. Targeted apoptosis of myofibroblasts with the BH3 mimetic ABT-263 reverses established fibrosis. Science translational medicine 9.
Latif, N., Quillon, A., Sarathchandra, P., McCormack, A., Lozanoski, A., Yacoub, M.H., Chester, A.H., 2015. Modulation of human valve interstitial cell phenotype and function using a fibroblast growth factor 2 formulation. PLoS One 10, e0127844.
Linge, C., Richardson, J., Vigor, C., Clayton, E., Hardas, B., Rolfe, K., 2005. Hypertrophic scar cells fail to undergo a form of apoptosis specific to contractile collagen-the role of tissue transglutaminase. J Invest Dermatol 125, 72-82.
Liu, M.M., Flanagan, T.C., Lu, C.C., French, A.T., Argyle, D.J., Corcoran, B.M., 2015. Culture and characterisation of canine mitral valve interstitial and endothelial cells. Vet J 204, 32-39.
Lu, C.C., Liu, M.M., Clinton, M., Culshaw, G., Argyle, D.J., Corcoran, B.M., 2015a. Developmental pathways and endothelial to mesenchymal transition in canine myxomatous mitral valve disease. Vet J.
Lu, C.C., Liu, M.M., Culshaw, G., Clinton, M., Argyle, D.J., Corcoran, B.M., 2015b. Gene network and canonical pathway analysis in canine myxomatous mitral valve disease: a microarray study. Vet J 204, 23-31.
Lu, C.C., Liu, M.M., Culshaw, G., French, A., Corcoran, B., 2016. Comparison of cellular changes in Cavalier King Charles spaniel and mixed breed dogs with myxomatous mitral valve disease. J Vet Cardiol 18, 100-109.
Markby, G., Summers, K.M., MacRae, V.E., Del-Pozo, J., Corcoran, B.M., 2017a. Myxomatous Degeneration of the Canine Mitral Valve: From Gross Changes to Molecular Events. J Comp Pathol 156, 371-383.
Markby, G.R., Summers, K.M., MacRae, V.E., Corcoran, B.M., 2017b. Comparative Transcriptomic Profiling and Gene Expression for Myxomatous Mitral Valve Disease in the Dog and Human. Vet Sci 4.
Plati, J., Bucur, O., Khosravi-Far, R., 2011. Apoptotic cell signaling in cancer progression and therapy. Integr Biol (Camb) 3, 279-296.
Surachetpong, S., Jiranantasak, T., Rungsipipat, A., Orton, E.C., 2013. Apoptosis and abundance of Bcl-2 family and transforming growth factor beta1 signaling proteins in canine myxomatous mitral valves. J Vet Cardiol 15, 171-180.
Tan, K., Markby, G., Muirhead, R., Blake, R., Bergeron, L., Fici, G., Summers, K., Macrae, V., Corcoran, B., 2019. Evaluation of canine 2D cell cultures as models of myxomatous mitral valve degeneration. PLoS One 14, e0221126.
Wang, S., Konorev, E.A., Kotamraju, S., Joseph, J., Kalivendi, S., Kalyanaraman, B., 2004. Doxorubicin induces apoptosis in normal and tumor cells via distinctly different mechanisms. intermediacy of H(2)O(2)- and p53-dependent pathways. The Journal of biological chemistry 279, 25535-25543.
Whitney, J.C., 1974. Observations on the effect of age on the severity of heart valve lesions in the dog. J Small Anim Pract 15, 511-522.
Willems, I.E., Havenith, M.G., De Mey, J.G., Daemen, M.J., 1994. The alpha-smooth muscle actin-positive cells in healing human myocardial scars. Am J Pathol 145, 868-875.
Yang, V.K., Tai, A.K., Huh, T.P., Meola, D.M., Juhr, C.M., Robinson, N.A., Hoffman, A.M., 2018. Dysregulation of valvular interstitial cell let-7c, miR-17, miR-20a, and miR-30d in naturally occurring canine myxomatous mitral valve disease. PLoS One 13, e0188617.

441